

Analytical Methods

Accepted Manuscript



This is an *Accepted Manuscript*, which has been through the Royal Society of Chemistry peer review process and has been accepted for publication.

Accepted Manuscripts are published online shortly after acceptance, before technical editing, formatting and proof reading. Using this free service, authors can make their results available to the community, in citable form, before we publish the edited article. We will replace this *Accepted Manuscript* with the edited and formatted *Advance Article* as soon as it is available.

You can find more information about *Accepted Manuscripts* in the [Information for Authors](#).

Please note that technical editing may introduce minor changes to the text and/or graphics, which may alter content. The journal's standard [Terms & Conditions](#) and the [Ethical guidelines](#) still apply. In no event shall the Royal Society of Chemistry be held responsible for any errors or omissions in this *Accepted Manuscript* or any consequences arising from the use of any information it contains.

A fast and highly sensitive method for the detection of canine distemper virus by naked eye

Caroline R. Basso^a, Claudia C. Tozato^b, João Pessoa A. Junior^b, Valber A. Pedrosa^{a*}

^a*Department of Chemistry and Biochemistry, Institute of Bioscience, UNESP-Botucatu, SP 18618-000, Brazil.*

^b*Department of Microbiology and Immunology, Institute of Bioscience, UNESP-Botucatu, SP 18618-000, Brazil.*

An easy, low cost method for the detection of canine distemper virus (CDV) that requires no instrumentation and uses gold nanoparticle-labeled antibodies is presented. The proposed method provides linear results between the concentration and signal in the range of 0 to 1.5 µg/L with a detection limit of 0.7 ng/mL. The method was successfully applied in the detection of the CDV virus in real samples of urine and, the results from these studies correlate with values obtained using conventional methods. Our results offer the possibility of easy, rapid and reliable clinical diagnosis of CDV by monitoring the colorimetric change and measuring linear surface plasmon resonance (LSPR) changes in urine samples. The rapid visual detection of the virus on a test assay may offer a simple and cost-effective alternative to highly complex and instrument-dependent commercial methods.

AUTOR INFORMATION

*Corresponding authors. Tel: +55 14 38800576.

Email addresses: vpedrosa@ibb.unesp.br (V.A. Pedrosa)

1
2
3 The canine distemper virus (CDV) is a highly contagious disease.¹ This pathogen has
4 high rates of mortality with lower mortality rates observed only in cases of canine
5 rabies,² but the eradication of this virus is considered impossible because of its wide
6 range of hosts, which includes terrestrial carnivores. However, CDV can be
7 prevented through vaccination. The high mortality rate of CDV necessitates the
8 acceleration of diagnostic procedures to quarantine infected individuals and start the
9 appropriate treatment early.³ The broad spectrum of clinical signs, which are similar to
10 the signs observed in other respiratory and enteric diseases of dogs, hampers clinical
11 diagnosis of canine distemper and requires laboratory confirmation. Some techniques
12 used to diagnose CDV include serology tests,⁴ indirect fluoroimmunoassay,⁵
13 histopathology,⁶ reverse transcription-polymerase chain reaction (RT-qPCR),⁴
14 immunofluorescence⁷ and immunohistochemistry.⁸ However, each of these tests has
15 limitations. The serological techniques are limited only allowing diagnosis of CDV
16 once the infected animal died from distemper and may or may not provide measurable
17 antibody titers.^{9,10} The technique of virus isolation in cell culture is specific but time-
18 consuming and can result in false-positive results if the animal is not in the acute phase
19 of the disease.⁵ Histopathology is not specific and normally requires a confirmatory test.
20 All of these techniques have the additional limitations of high cost, being time-
21 consuming and requiring extraction of nucleic acids and genome amplification using
22 polymerase chain reaction (PCR) or RT-PCR.

23
24
25
26
27
28
29
30
31
32
33
34
35
36
37 More recently, metallic nanoparticles have been successfully employed as molecular-
38 recognition elements and amplifier biosensors, in addition to serving as components in
39 nanoscale optical devices.⁶ Immunoassays using gold nanoparticles have attracted much
40 attention because of their size- and shape-dependent optical properties, which differ
41 significantly from those of the bulk metals.¹¹ Gold nanoparticles are of great interest for
42 label-free sensing because their extinction spectrum is highly sensitive to the dielectric
43 constant of the surrounding medium.¹² According *Selvakumar et al.*, gold nanoparticles
44 are ideal materials for the production of biosensors since they present between all
45 unique electronic and optical properties, making them suitable for application in
46 immunoassays.¹³ Biosensors using gold nanoparticles are more easier and stable to
47 work than those using a conventional system with enzymes or fluorescent, so that they
48 are bioconjugation easily with various ligands such as nucleic acids, aptamers and
49 anticorpos.¹⁴⁻¹⁶ Localized surface plasmon resonance (LSPR) biosensors employ noble
50 metal nanoparticles as an alternative to surface plasmon resonance (SPR) sensors
51
52
53
54
55
56
57
58
59
60

1
2
3 because the highly localized electromagnetic fields that occur at nanoparticle surfaces
4 can enable improved detection of nanoscale biological analytes. LSPR can sensitively
5 monitor binding events in real time and has been used to detect a variety of processes,
6 including biomolecular interactions (antigen–antibody, DNA–DNA, protein–enzyme),
7 and for typical detection times. Also, the LSPR peak position is strongly dependent on
8 the size and shape of the nanoparticles, as well as on the dielectric constant of the
9 environment. It was previously demonstrated that changing the interparticle distance
10 radically changes the gold nanoparticle LSPR peak position. Normally gold
11 nanoparticles show a maximum absorption at ca. 520 nm. After the bioconjugation, they
12 start forming aggregates, which shifts the absorption band to ca. 600–800 nm. This
13 change can be observed by the naked eye or measured quantitatively with an ultraviolet-
14 visible (UV–Vis) spectrophotometer. This behavior has been utilized for sensing of
15 various biological substances and models such as immunoglobulin,¹⁵ Alzheimer’s
16 disease,¹⁶ *E. coli* and salmonella,¹⁷ nuclease activity,¹⁸ DNA,¹⁹ influenza virus²⁰ and
17 bacteriophages.²¹

18
19 In this study, we describe a simple and colorimetric new method to detect CDV,
20 using real-time binding of an antigen to an antibody-gold-nanoparticle conjugate. In
21 contrast to the previously mentioned conventional methods for the detection of CDV,
22 the methodology provides a convenient means of realizing rapid and sensitive CDV-
23 specific antibody detection. In addition, this methodology is fast, non-toxic, and
24 biocompatible and can partially mimic conditions in whole serum samples for clinical
25 use, as compared to conventional ELISA-based protocols. The great advantage of this
26 new method is that the samples used for diagnosis are urines collected in a non invasive
27 manner not being painful for the animal. Another advantage of this technique as
28 compared to other existing is that based on a colorimetric analysis using gold
29 nanoparticles which have unique characteristics compared with other materials, such as
30 unique ability to good biocompatibility and easy functionalization with proteins that
31 make them ideal as labeling tags or reading platforms in biosensors.²²

32
33 Antibody immobilization on the gold nanoparticles (AuNPs) was investigated using
34 LSPR spectroscopy. Antibodies were labeled with 25-nm AuNPs through electrostatic
35 and covalent interactions between the antibody side chains and nanoparticle surfaces.
36 AuNPs were synthesized according to standard wet chemical methods using sodium
37 citrate as a reducing agent.²³ A colloidal gold solution appears intensely red in color. The
38 transition electron microscopy (TEM) image in Figure S1A shows mono dispersed gold
39
40
41
42
43
44
45
46
47
48
49
50
51
52
53
54
55
56
57
58
59
60

1
2
3 nanoparticles with an average particle diameter of 23 nm (see Figure S1B). A
4 characteristic LSPR band of the AuNPs is shown in the UV-Vis spectrum at 525 nm,
5 which confirms the presence of nanoparticles (see Figure S1C). To verify that the
6 antibodies are attached to the gold nanoparticles, extinction measurements of the gold
7 nanoparticles were taken before and after the conjugation step (Figure 1A). The gold
8 nanoparticles exhibited an extinction peak at 525 nm. The next step of the method led to
9 a peak that shifted 6 nm, indicating the self-assembled monolayer modification. The
10 representative LSPR peak after the treatment with 1:1 EDC/NHS shifted to 533 nm
11 (green line). Following antibody conjugation, the extinction peak shifted to 616 nm,
12 indicating the attachment of the antibody. This shift is attributed to an increase in the
13 local refractive index due to the antibody and is the result of an increase in the local
14 refractive index of the medium surrounding the gold nanoparticles, as shown in the blue
15 line. When the anti-CDV conjugated gold nanoparticles were measured, the LSPR band
16 intensity decreased and continued to remain lower than that of the LSPR bands before
17 the addition of anti-CDV. This behavior is caused by the interaction of the antibody
18 with the colloidal gold particles. The agglutination of the gold probe with the anti-CDV
19 antibody IgG reduces the surface of nanoparticles; consequently, the surface plasmon
20 resonance is decreased. In comparing the nanoparticle spectra before and after antibody
21 immobilization, there was a displacement of the peak at 97 nm because the ratio of the
22 LSPR peak increases when the samples are illuminated with unpolarized light. This
23 change in the optical spectrum suggests that some of the nanoparticles may be attached
24 in an end-on configuration. Following CDV conjugation there was an extinction peak
25 shift of 30 nm. As shown in Figure 1B, a clear colorimetric change is observed when
26 CDV was added to the antibody-conjugated gold nanoparticles. This colorimetric
27 change is mainly due to the aggregation of the antibody-conjugated gold nanoparticles,
28 as shown in Figure 1A, followed by an extinction peak shift of 30 nm. We have not
29 observed any color change upon the addition of serum albumin (BSA) protein or the
30 negative control (see supporting Figure S2B). The colorimetric data demonstrate that
31 our assay is highly sensitive to CDV and can distinguish it from other proteins. All the
32 experiment, since from the preparation of solutions to be used to the adsorption of the
33 urine sample, lasted about 2:30 hours.

34
35
36
37
38
39
40
41
42
43
44
45
46
47
48
49
50
51
52
53
54
55
56
57
58
59
60
The observations of the LSPR band changes were further confirmed through the
characterization of each step of the experiment using transmission electron microscopy
(TEM). To perform the analysis, each solution was deposited in specific metals gratings

1
2
3 of equipment and was viewed on the day after its deposition, in order to completely dry,
4 thereby excluding possible interfering. Figure 2A(A) shows a representative TEM
5 image of the gold nanoparticles with average diameter of 25 nm. After modification
6 with MUA and EDC/NHS, the nanoparticles were measured to have a diameter of 48
7 nm (Figure 2A(B)), which confirmed an increase in shell thickness. Figure 2A(C) show
8 the adsorption of the antibody through covalent binding between the thiol groups and
9 the amines present in the antibody. After the interaction between the antibody and CDV,
10 the nanoparticles have a diameter of 200 nm because CDV is very large with a diameter
11 of approximately 100 nm (Figure 2A(D)). Comparing the results obtained using UV-Vis
12 spectrometry and its reduction in the intensity of peak absorbance, we conclude that the
13 results are consistent with the images observed using TEM. Our TEM image shows
14 clearly that the antibody-conjugated gold nanoparticle and CDV interaction is highly
15 specific. As a result, a colorimetric change is observed from red to yellow in color (as
16 shown in Figure 1B). To confirm the results obtained in the characterization through
17 TEM, we realize all the experimental step using surface plasmon resonance (SPR).
18 Analyzing the SPR graphic (Figure 2B), we can observe all binding process which
19 occurs throughout the experiment. The point A is the injection of EDC/NHS on the gold
20 surface of the sensor that is modified with MUA, after this step washing of the surface
21 was performed using a phosphate buffer solution pH 7.4 to remove weakly bound
22 material (point B). In the point C was added to the antibody solution that remained for
23 1h, followed by washing (point D). To subtract the point D to point C, we can see that
24 there was a shift in the RU for 301.24 milledegree with correspond to 2.5 ng/mm² of
25 antibody adsorbed in gold nanoparticles, because an increase in the plasmon resonance
26 angle of 120 millidegrees corresponds to an average material layer growth of 1 ng
27 mm⁻².²⁴ After this washing step, we can observe that there was a small decay in the
28 graph compared to the baseline (point C to D) confirming that there was a link between
29 the antibody and nanoparticles. Point E represents the injection of BSA solution used to
30 block the remaining spaces between antibodies, followed by washing (point F). The
31 point G is the injection of negative urine (negative control), after the washing process it
32 is possible to observe that there was a total decay of the line equaling the baseline,
33 confirming the negative control (points G to H). The regeneration of the sensor surface
34 was performed using glycine solution, which removed all the antigen prevailing only
35 binding until antibodies, followed by washing steps (points I and M to J and N). The
36 injection of positive sample with the presence of the virus occurred at points K and O,
37
38
39
40
41
42
43
44
45
46
47
48
49
50
51
52
53
54
55
56
57
58
59
60

1
2
3 which after the washing in points L and P, occurred a small decay signal showing that
4 occurred specific binding between the antigen/antibody. All washing steps were
5 performed using phosphate buffer solution pH 7.4.
6
7

8 To determine the optimal concentration of antibodies for the experiment, tests
9 varying the dilutions of the antibody were performed (see Figure S3A). The ability of
10 these gold nanoparticle-conjugated antibodies to bind specifically to an antigen and
11 enhance the LSPR sensor response was measured by monitoring the LSPR shift upon
12 antibody binding at several different concentrations of CDV. Hence, the sensitivity of
13 the methodology was examined (Figure 3A); a plot of the changes in absorbance as a
14 function of the anti-IgG concentration shown in Figure 3B indicates that the CDV
15 detection limit was 0.7 ng/mL. Within the insert in the figure, the linear range of the
16 CDV concentration as well as the linear fit of the plotted graph is shown (Figure 3B).
17 The relative standard deviation (RSD) is 6.5%, showing a good reproducibility of the
18 immunosensor preparation. The LSPR band intensity of the gold nanoparticles
19 decreased and continued to remain lower than that of the LSPR bands before the
20 addition of anti-CDV (Figure 5A). This observation is due to the fact that the CDV is
21 much larger in size (~100nm) than the gold-nanoparticle bioprobes modified by the
22 anti-CDV antibody (88 nm), and several antibody-conjugated gold nanoparticles are
23 attached to the CDV surface. A similar result was also reported by *Wang and*
24 *Irudayaraj* through varying the concentration of *E. coli*, in which a higher concentration
25 of the sample had a smaller absorbance intensity and higher scattering due to the large
26 number of compounds present in the sample. Similar behavior of IgG was found with
27 CDV; the absorbance signal decreases as the CDV concentration increases. This
28 indicates excellent sensitivity for a plasmonic nanosensor.^{25,26} We normalized each pair
29 of spectra to the absorbance at the maximum extinction before CDV attachment, which
30 allowed for an easy comparison of the relative extinction increases after CDV
31 attachment for each pair with the aim of exploring the selectivity for Au-LSPR. Similar
32 virus needs to be seriously considered because they could be provided a false positive
33 response. We investigated the effects of Ophidian Paramyxovirus (OPMV) (1),
34 Parvovirus (2) Paramyxovirus (3), and Newcastle virus (4) on the immunosensor
35 response (see Figure 1). There was no change of color for all virus tested. These results
36 demonstrate that the methodology was selective to CDV in the presence of other similar
37 virus.
38
39
40
41
42
43
44
45
46
47
48
49
50
51
52
53
54
55
56
57
58
59
60

1
2
3 To evaluate the practicality of the methodology using gold nanoparticle-labeled
4 antibodies, our results were compared with pre-existing nested RT-qPCR methodology
5 using 14 positive urine samples. The average positive hits are in the range of 98.0%,
6 which further indicates that the developed immunosensor possesses an excellent
7 specificity and its performance meets the requirements for a sensitive determination of
8 CDV in urine samples. This methodology has the potential to provide rapid and
9 valuable information of presence of CDV as an alternative to time-consuming and
10 expensive instrumentation analysis.
11
12
13
14
15
16

17 **Conclusions**

20
21 In this work, we demonstrate the simple synthesis of gold nanoparticles modified for the
22 detection of CDV. Binding of CDV resulted in a redshift in the LSPR absorption peak,
23 and a good correlation was observed between the wavelength shift and concentration,
24 which demonstrates the feasibility of the method for the quantitative measurement of
25 CDV. The method exhibited a linear range for CDV between 0 and 1.5 $\mu\text{g/mL}$ with a
26 lower detection limit of 0.7 ng/mL. The method has been shown to be simple, reliable,
27 sensitive, selective and cost-effective for the measurement of CDV in urine samples. The
28 most important characteristic of the method is direct detection by the “naked-eye”,
29 which makes it more convenient than other methods that rely on advanced
30 instrumentation. With the results obtained in this work, our future prospects are to
31 employ the use of this methodology for the diagnosis of other pathogens in different
32 areas as a food, environment, and medical research.
33
34
35
36
37
38
39
40
41
42

43 **Acknowledgments**

44
45
46 We gratefully acknowledge partial support by grants from the FAPESP (2014/05653-5,
47 2012/15666-1), CNPq and CAPES.
48
49
50
51
52
53
54
55
56
57
58
59
60

References

- 1 C.R. Basso, C.C. Tozato, M.C.M. Ribeiro, J.P. Araujo Junior, V.A. Pedrosa, *Anal. Methods*. 2013, **5**, 5089-5094.
- 2 S.L. Deem, L.H. Spelman, R.A. Yates, R.J. Montali, *J. Zoo Wild. Med* 2000, **31**, 441-451.
- 3 A. Beineke, C. Puff, F. Seehusen, W. Baumgartner, *Vet. Immunol. Immunopathol.* 2009, **127**, 1-18.
- 4 N. Santos, C. Almendra, L. Tavares, *J. Wildl. Dis.* 2009, **45**, 221-226.
- 5 Y. Shin, T. Mori, M. Okita, *J. Vet. Med. Sci.* 1995, **57**, 439-445.
- 6 E. Hutterand, J.H. Fendler, *Adv. Mater.* 2004, **16**, 1685-1706.
- 7 A. Józwick, T. Frymus, *T. Vet. Res. Commun.* 2005, **29**, 347-359.
- 8 P. Schmidt, A. Hafner, G.H. Reubel, R. Wanke, V. Franke, U. Losch, E. Dahme, *J. Vet. Med. Ser. B.* 1989, **36**, 661-668.
- 9 M.J.G. Appel, *Am. J. Vet. Res.* 1969, **30**, 1167-1182.
- 10 A.L., Frisk, M. Konig, A. Moritz, *A. J. Clin. Microbiol.* 1999, **37**, 3634-3643.
- 11 A.J. Haes, D.A. Stuart, S. Nie, R.P.J. Van Duyne, *J. Fluoresc.* 2004, **14**, 355-367.
- 12 S.M. Marinakos, S. Chen, A. Chilkoti, *Anal. Chem.* 2007, **79**, 5278-5283.
- 13 L.S. Selvakumar, K.V. Ragavan, K.S. Abhijith, M.S. Thakur, *Anal. Methods*. 2013, **5**, 1810.
- 14 G.D. Richards, *Anal. Biochem.* 1996, **236**, 170.
- 15 D.P. Tang, Y.L. Cui, G.A. Chen, *Analyst*, 2013, **138**, 981.
- 16 X.D. Cao, Y.K. Ye, S.Q. Liu, *Anal. Biochem.* 2011, **417**, 1.
- 17 Z. Ma, S.F. Sui, *Angew. Chem. Int. Ed.* 2002, **41**, 2179.
- 18 J. Haes, L. Chang, W.L. Klein, R.P. Van Duyne, *J. Am. Chem. Soc.* 2005, **127**, 2264-2271.
- 19 C. Wang, J. Irudayaraj, *Small*. 2008, **12**, 2204-2208.
- 20 Y. Li, H.J. Lee, R.M. Corn, *Anal. Chem.* 2007, **79**, 1082-1088.
- 21 T. Endo, K. Kerman, N. Nagatani, Y. Takamura, E. Tamiya, *Anal. Chem.* 2005, **77**, 6976-6984.
- 22 X. Wang, Y.L.H. Wang, Q.F.J. Peng, Y. Wang, J. Du, Y. Zhou, L. Zhan, *Biosens. Bioelectron.* 2010, **26**, 404-410.

- 1
2
3 23 A. Lensniewski, M. Los, M.J. Niedziolka, A. Krajewska, K. Szot, J.M. Los, J.N.
4 Jonsson, *Bioconjugate Chem.* 2014, **25**, 644-648.
5
6 24 Seow, N., Lai, P.S., Yung, L.Y.L. *Anal. Biochem.* 2014, **451**, 62.
7
8 25 <http://www.metrohm.hu/DownloadsDocs/App1010.pdf>
9
10 26 J.N. Anker, W.P. Hall, O. Lyandres, N.C. Shah, J. Zhao, R.P. Van Duyne, *Nat.*
11 *Mater.* 2008, **6**, 453.
12
13 27 J. Homola, S.S. Yee, G. Gauglitz, G. *Sens. Actuators, B.* 1999, **54**, 3-15.
14
15 28 A.D. McFarland, C.L. Haynes, C.A. Mirkin, R.P. Van Duyne, H.A. Godwin, *J.*
16 *Chem. Education.* 2004, **81**, 544.
17
18
19
20
21
22
23
24
25
26
27
28
29
30
31
32
33
34
35
36
37
38
39
40
41
42
43
44
45
46
47
48
49
50
51
52
53
54
55
56
57
58
59
60

Figure Caption

Fig. 1 UV-Vis spectrum showing the absorbance and wavelength of the sample of gold nanoparticles (black line), MUA (red line), EDC / NHS (green line), antibody (blue line) and CDV (pink line). The colorimetric tests show gold nanoparticles (A), after addition of antibody (B), a positive sample (C) and a negative sample (D), respectively. Inteferent test: Ophidian Paramyxovirus (OPMV) (1), Parvovirus (2) Paramyxovirus (3), and Newcastle virus (4).

Fig. 2 A) TEM images of gold nanoparticles (A) and gold nanoparticles modified with self assembled-monolayer (B), antibody (C) and CDV (D). **B)** SPR graph showing the steps of the experiment and all process of adsorption and desorption on the surface of the sensor. The point A is injection of EDC/NHS, point C is adsorption of antibody, point E is solution of BSA, point G is injection the negative urine sample (negative control), points I was the glycine injections, K was the positive urines samples with the presence of CDV virus and the points B, D, F, H, J, and L are the washing steps using phosphate buffer pH 7.4.

Fig. 3 Variations of the CDV concentrations. A) A sample of CDV diluted in 1 mL of $100.0 \mu\text{g L}^{-1}$ in 10 mM PBS to 0.0 mL PBS (pink line), 20.0 mL PBS (black line), 50.0 mL PBS (red line), 100.0 mL PBS (green line) and 150.0 mL PBS (blue line). B) Calibration curve for CDV.

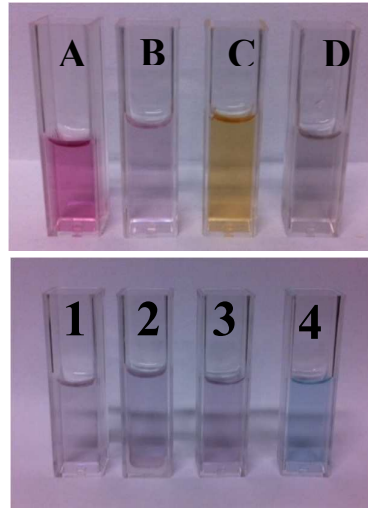
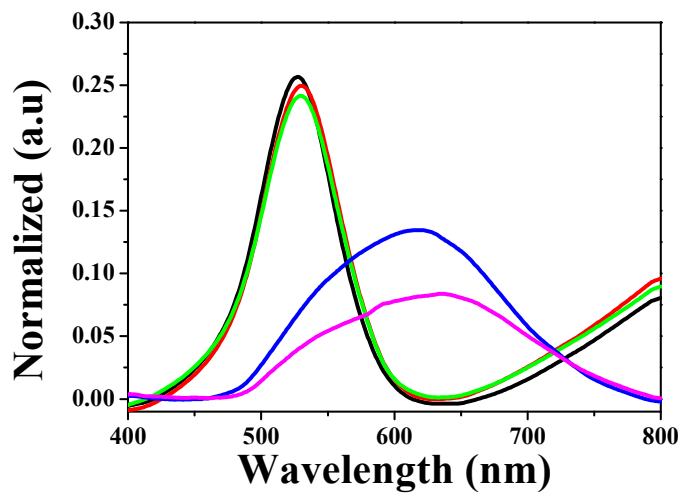


Fig 1.

1
2
3
4
5
6
7
8
9
10
11
12
13
14
15
16
17
18
19
20
21
22
23
24
25
26
27
28
29
30
31
32
33
34
35
36
37
38
39
40
41
42
43
44
45
46
47
48
49
50
51
52
53
54
55
56
57
58
59
60

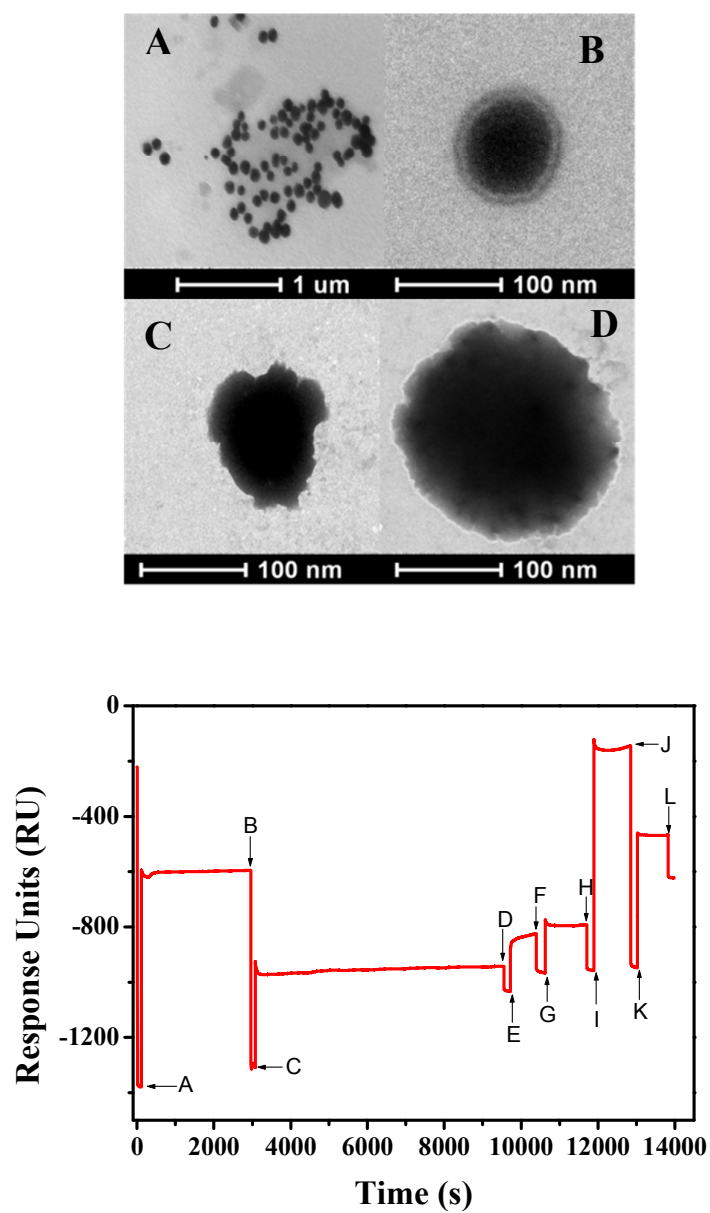


Fig. 2.

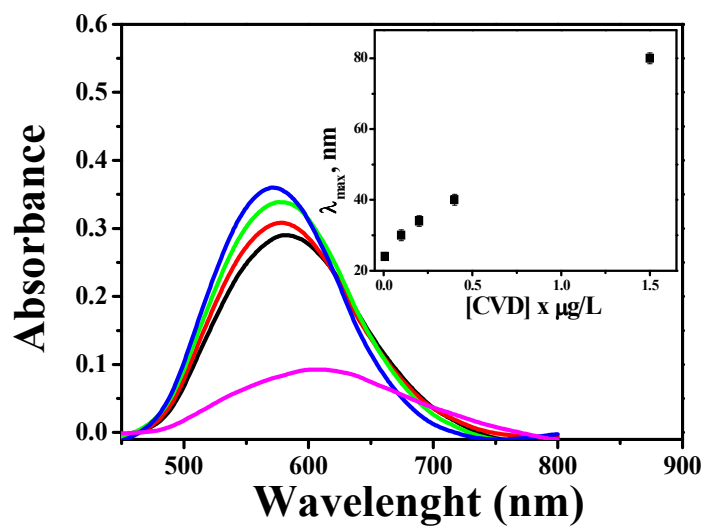


Fig. 3.